

Optimization and Heuristics for Cognitive Radio Design

Bharath Keshavamurthy

School of Electrical and Computer Engineering, Purdue University

22 April, 2020

Outline

- ▶ Motivation
- ▶ The DARPA SC2 radio
- ▶ Spectrum sensing and access via approximate POMDPs
- ▶ Implementation feasibility analysis on ESP32 radios

Motivation (1/2)

THE WALL STREET JOURNAL.

TECH

Wireless Companies Share the Airwaves

New cellular service lets the military, companies and others use the same frequencies—provided they don't interfere with each other

WSJ | OPINION

OPINION | LETTERS

U.S. Needs Better Spectrum Policy to Win in 5G World

To speed up 5G, we need to throw out spectrum auctions entirely.

Feb. 7, 2020 1:13 pm ET

WSJ | OPINION

OPINION | BUSINESS WORLD

How Government Can Get Brave About Spectrum

Ignore the groups that gripe about a taxpayer rip-off. The public benefits when airwaves trade freely.



By [Holman W. Jenkins Jr.](#)

June 14, 2019 6:41 pm ET

Motivation (2/2)



THE WALL STREET JOURNAL

THE SATURDAY ESSAY

The Ultimate Learning Machines

The future of artificial intelligence depends on designing computers that can think and explore as resourcefully as babies do.

A photograph of a baby looking up at a large, metallic humanoid robot.

DARPA SC2: Problem Statement

- ▶ Multi-agent resource allocation
- ▶ Centralized setting
- ▶ Incumbents and Competitors
- ▶ Max our network's scores
- ▶ Ensure min mandated performance of ensemble

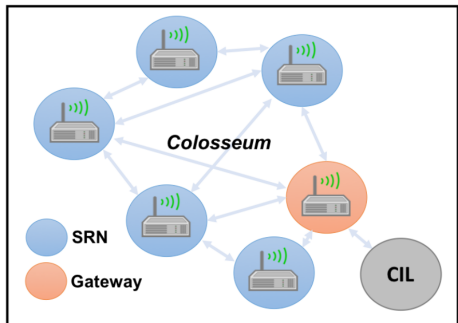


Figure 1: The CIRN architecture

Related Work: DARPA SC2 Competitors

- ▶ **SCATTER**¹: OFDM waveform, McF-TDMA, Distributed channel allocation, Target-score based flow scheduling
- ▶ **Zylinium**²: OFDM PHY, CIL-based centralized channel allocation, Mixed integer programming for flow scheduling

¹Giannoulis, et. al., "The SCATTER approach...", 2019 IEEE DySPAN

²R.J. Baxley, R.S. Thompson, "Team Zylinium...", 2019 IEEE DySPAN

Challenges: Our Design Principles

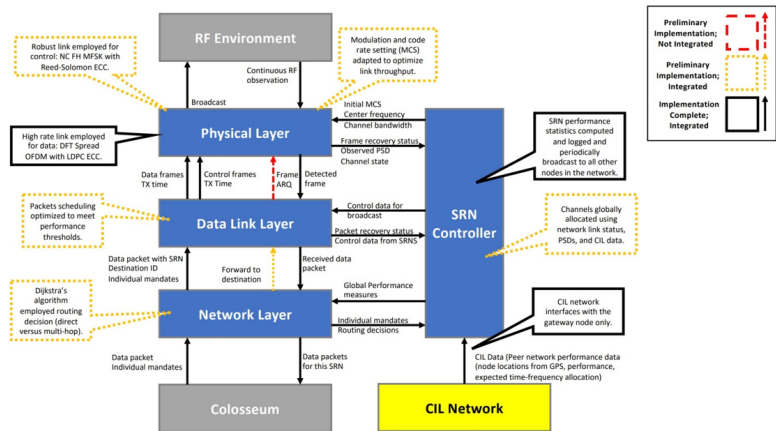


Figure 2: Our radio's network protocol stack³

³Contributions: DLL, Scoring, PSD+Collab, CIL, GUI

PHY: Transmission Power Control (1/3)

- ▶ Collaborate to ensure incumbent interference compliance
- ▶ **Violation:** Aggregate interference at the incumbent exceeds current threshold
- ▶ **Reduce Tx power** of all SRNs proportionate to the excess interference divided by number of SRNs

PHY: Transmission Power Control (2/3)

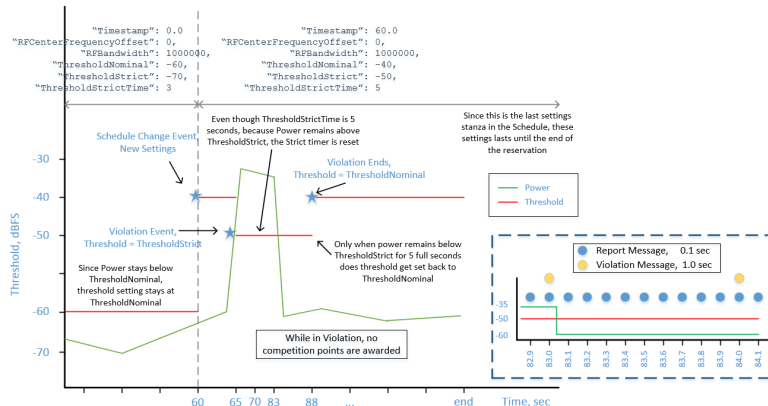


Figure 3: The temporal behavior of the **Passive Incumbent**⁴

⁴ DARPA Colosseum

PHY: Transmission Power Control (3/3)

The screenshot displays a network monitoring interface with three main sections: Message List, Filters, and Event Log.

Message List: A vertical list of log entries, many of which are highlighted in green. The visible entries include:

- (458.1) incumbent_notify
- (458.2) location_update
- (458.3) detailed_performance
- (458.2) incumbent_notify
- (458.3) incumbent_notify
- (458.4) incumbent_notify
- (458.5) incumbent_notify
- (458.6) incumbent_notify
- (458.7) incumbent_notify
- (458.8) incumbent_notify
- (458.9) incumbent_notify
- (458.10) incumbent_notify
- (458.11) incumbent_notify
- (458.12) incumbent_notify
- (458.13) incumbent_notify
- (458.14) incumbent_notify
- (458.15) incumbent_notify
- (458.16) incumbent_notify
- (458.17) incumbent_notify
- (458.18) incumbent_notify
- (458.19) incumbent_notify
- (458.20) incumbent_notify
- (458.21) incumbent_notify
- (458.22) spectrum_usage
- (458.23) incumbent_notify
- (458.24) incumbent_notify
- (458.25) incumbent_notify
- (458.26) incumbent_notify
- (458.27) incumbent_notify
- (458.28) incumbent_notify

Filters: A section containing two dropdown menus. The first dropdown is set to "Collaboration" and the second dropdown contains the value "172.30.200.191".

Message View: A detailed view of a selected message entry. The message content is as follows:

```
sender_network_id: 172.30.200.191
msg_count: 5034
timestamp {
    seconds: 1567487004
    picoseconds: 105668000000
}
network_type {
    network_type: INCUMBENT_PASSIVE
}
incumbent_notify {
    data {
        incumbent_id: 191
        msg_type: VIOLATION
        report_time {
            seconds: 1567487004
            picoseconds: 105089000000
        }
        power: -73.53056193276363
        threshold: -75.0
        center_freq: 1000000000
        bandwidth: 4000000
        threshold_exceeded: true
    }
}
```

Event Log: A list of log entries showing state changes and peer additions. The visible entries are:

- [4581.6] State change from NO_STATE to INIT.
- [4581.6] Connection attempt. Success
- [4581.6] State change from INIT to REGISTER.
- [4581.5] State change from REGISTER to REGISTER_WAITING.
- [4581.2] Added peer 172.30.200.191
- [4581.2] State change from REGISTER_WAITING to ACTIVE.

Figure 4: A **Violation** collaboration message from the Passive Incumbent

PHY: The FSK Control Channel (1/2)

- ▶ Short control frames
- ▶ Initial node discovery; Fallback link
- ▶ Non-coherent 8-FSK link with 480kHz of bandwidth
- ▶ Slotted ALOHA (without CD and backoff)

PHY: The FSK Control Channel (2/2)

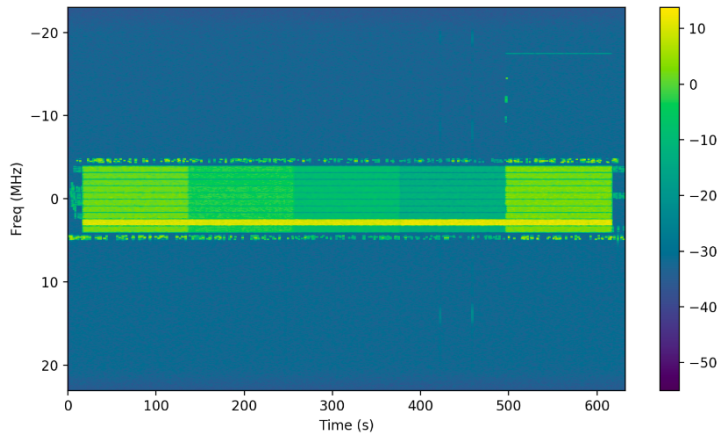


Figure 5: The center frequency switches between the upper and lower spectral band-edges during an SC2 Qual scenario

PHY: The DFT-s-OFDM Data Channel (1/2)

- ▶ Long control frames+traffic
- ▶ 128 sub-carriers: 108 for data, 12 for pilot, 8 for null transmissions
- ▶ Allowed modulation: QPSK, QAM16, QAM32, and QAM64
- ▶ Allowed code rates: $\frac{1}{2}$, $\frac{2}{3}$, $\frac{3}{4}$, and $\frac{5}{6}$ (IEEE 802.11 QC-LDPC)

PHY: The DFT-s-OFDM Data Channel (2/2)



Figure 6: The power spectrum of DFT-s-OFDM waveform

PHY: MCS Adaptation (1/3)

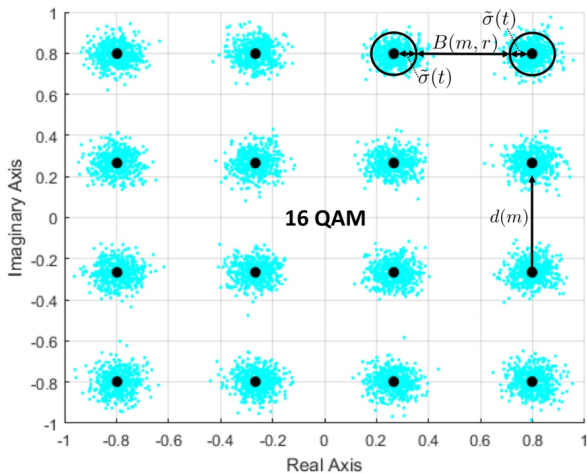


Figure 7: The MCS adaptation algorithm based on minimizing the distance between the circles centered at two adjacent constellation symbols

PHY: MCS Adaptation (2/3)

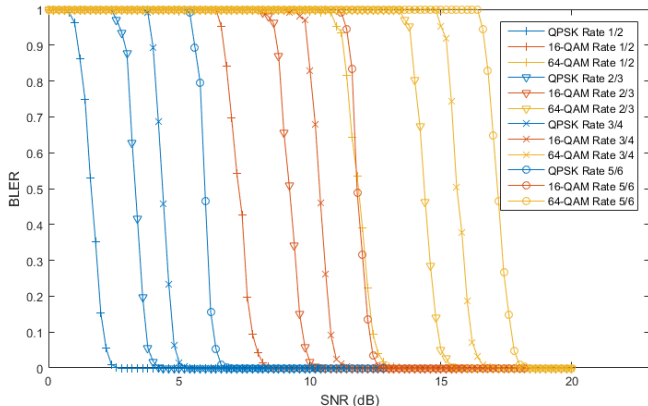


Figure 8: Simulated BLER curves for different combinations of modulation order and code rate

PHY: MCS Adaptation (3/3)

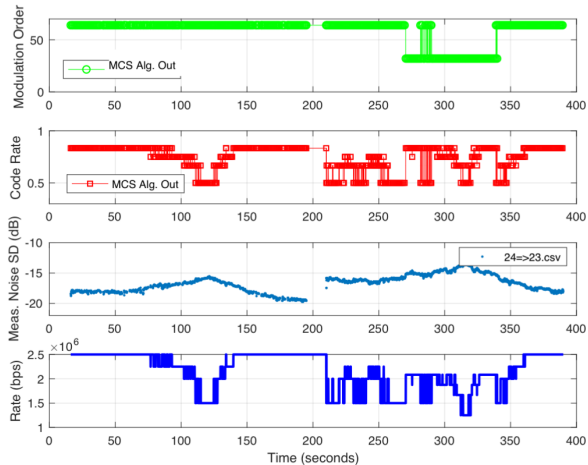


Figure 9: MCS adaptation to changes in noise variance during an SC2 Payline scenario

DLL: Prioritized Flow Scheduling with ARQ (1/4)

- ▶ VOIP=4, UAV CCTV stream=9, Video bombing run=15
- ▶ Find the UB and LB of a QS using flow info and link quality
- ▶ Rank the flows in the decreasing order of their value/resource
- ▶ Fit into the QS in the ranked order w/ recursive revisitaton

DLL: Prioritized Flow Scheduling with ARQ (2/4)

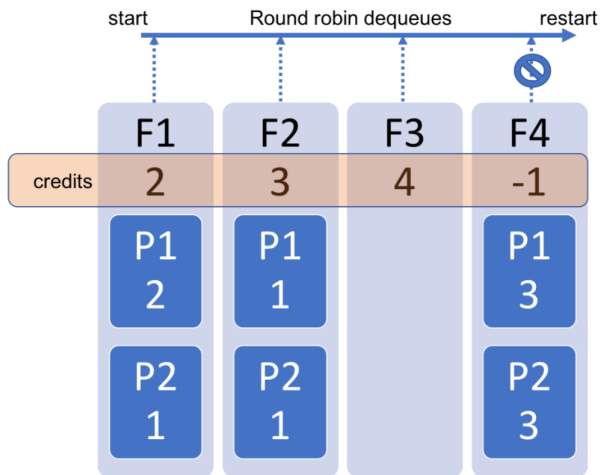


Figure 10: Deficit round-robin scheduling with a concept of “credits”

DLL: Prioritized Flow Scheduling with ARQ (3/4)

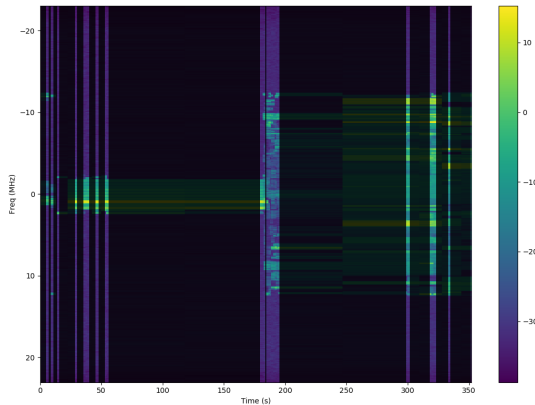


Figure 11: A situation in which PSD flows from an SRN (to the GW) are not prioritized over other flows during an SC2 Payline scenario

DLL: Prioritized Flow Scheduling with ARQ (4/4)

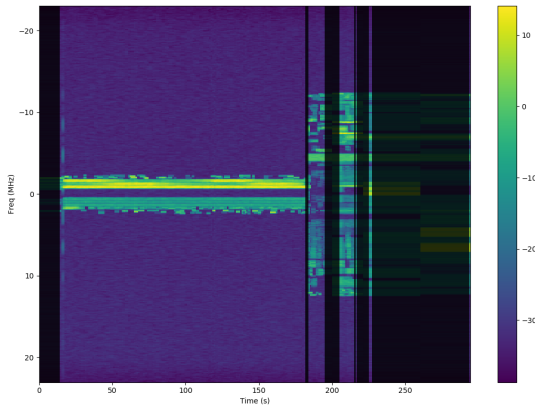


Figure 12: A situation in which PSD flows from an SRN (to the GW) are prioritized over most other flows during an SC2 Payline scenario: leads to a drop in scores

MAC: BW and Channel Allocation (1/3)

- ▶ BW : Traffic stats, QoS reqs, link quality, self & peer scores
- ▶ f_c : PSD obs, self & peer scores, GPS, Tx power
- ▶ A heuristic search to determine the center frequencies that minimize the interference at our SRN receivers

MAC: BW and Channel Allocation (2/3)

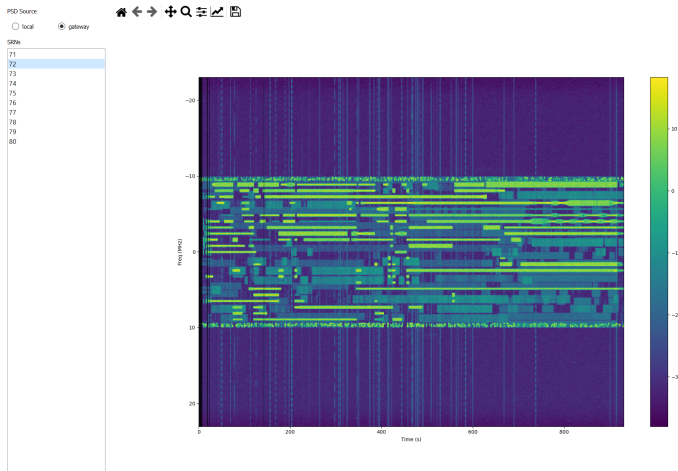


Figure 13: The PSD observations from SRN 72 to our GW during an SC2 Alleys of Austin scenario

MAC: BW and Channel Allocation (3/3)

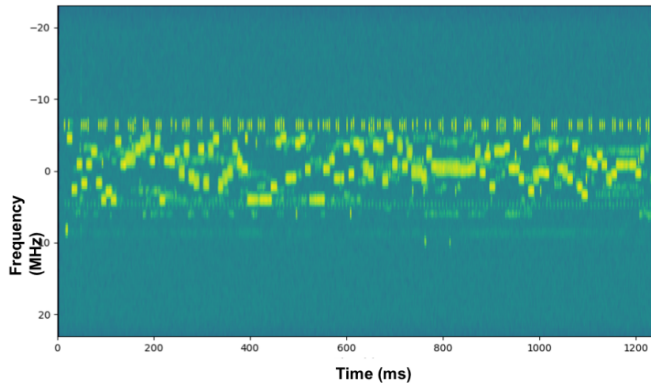


Figure 14: The spectrum occupied by our SRNs (time-frequency map) with re-allocations dictated by a combination of local PSD obs and CIL msgs, during an SC2 Alleys of Austin scenario

NET: Multi-hop Routing (1/3)

Binary link status vectors → Route tables → Dijkstra's algorithm

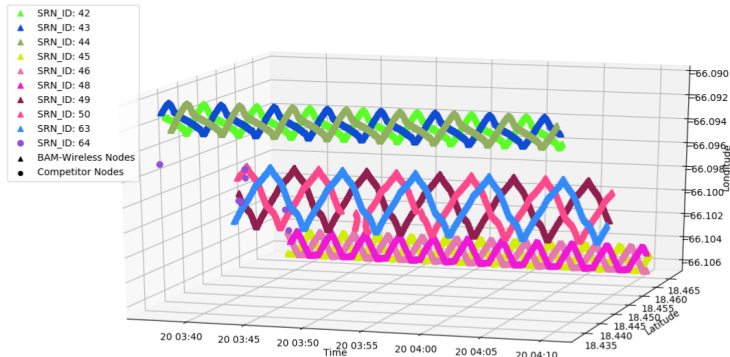
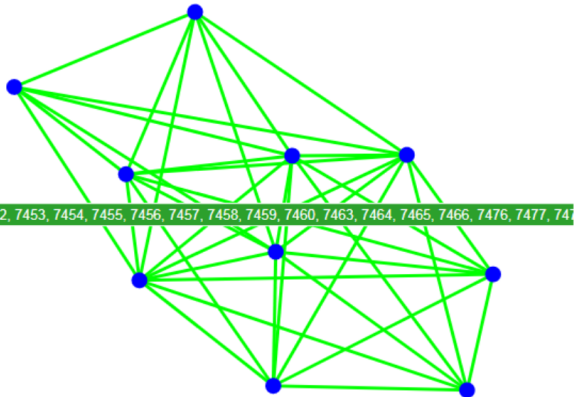


Figure 15: SRN mobility as emulated in an SC2 Payline scenario causes variations in RF propagation characteristics

NET: Multi-hop Routing (2/3)

Link-Flow Mapping Visualization using [RESERVATION-PAYLINE]



Link-Flow Mapping Visualization using [RESERVATION-PAYLINE]

Figure 16: Our **network map** in an SC2 Payline scenario

NET: Multi-hop Routing (3/3)

	1	Associated Flows	2	1	2
1	Links			135 5565	[50→51]
2	[55→58]	5002, 5001, 5003, 5271, 5272, 5273		136 5566	[50→51]
3	[55→54]	5541, 5542, 5543, 5811, 5812, 5813		137 5567	[50→51]
4	[55→52]	5545, 5544, 5546, 5814, 5815, 5816		138 5568	[50→49]
5	[49→58]	5018, 5016, 5017, 5280, 5286, 5287		139 5569	[50→49]
6	[49→50]	5576, 5574, 5575, 5845, 5844, 5846		140 5570	[50→49]
7	[49→51]	5573, 5571, 5572, 5841, 5842, 5843		141 5571	[49→51]
8	[45→58]	5026, 5027, 5025, 5296, 5295, 5297		142 5572	[49→51]
9	[45→48]	5590, 5591, 5589, 5859, 5861, 5860		143 5573	[49→51]
10	[45→46]	5592, 5593, 5594, 5862, 5863, 5864		144 5574	[49→50]
11	[48→58]	5019, 5020, 5021, 5290, 5289, 5291		145 5575	[49→50]
12	[48→46]	5578, 5577, 5579, 5848, 5847, 5849		146 5576	[49→50]
13	[48→45]	5581, 5580, 5582, 5850, 5851, 5852		147 5577	[49→46]
14	[54→58]	5006, 5005, 5004, 5275, 5274, 5276		148 5578	[48→46]
15	[54→52]	5552, 5550, 5551, 5820, 5821, 5822		149 5579	[48→46]
16	[54→55]	5549, 5547, 5548, 5817, 5818, 5819		150 5580	[48→45]
17	[52→58]	5008, 5009, 5007, 5277, 5278, 5279		151 5581	[48→45]
18	[52→55]	5554, 5553, 5555, 5821, 5824, 5825		152 5582	[48→45]
19	[52→54]	5557, 5558, 5556, 5826, 5827, 5828		153 5583	[46→48]
20	[58→46]	5051, 5049, 5050, 5319, 5320, 5321		154 5584	[46→48]
21	[58→45]	5053, 5054, 5052, 5322, 5323, 5324		155 5585	[46→48]
22	[58→48]	5047, 5046, 5048, 5316, 5317, 5318		156 5586	[46→45]
23	[58→50]	5040, 5041, 5042, 5310, 5312, 5311		157 5587	[46→45]
24	[58→49]	5043, 5044, 5045, 5313, 5314, 5315		158 5588	[46→45]
25	[58→51]	5038, 5037, 5039, 5308, 5307, 5309		159 5589	[45→48]
26	[58→52]	5036, 5034, 5035, 5306, 5304, 5305		160 5590	[45→48]
27	[58→54]	5032, 5031, 5033, 5301, 5302, 5303		161 5591	[45→48]
28	[58→53]	5030, 5028, 5029, 5280, 5289, 5300		162 5592	[45→46]

Figure 17: Link-Flow Mapping for our network in an SC2 Payline scenario

SC2 Wildfire: Disaster-Relief Scenario Analysis

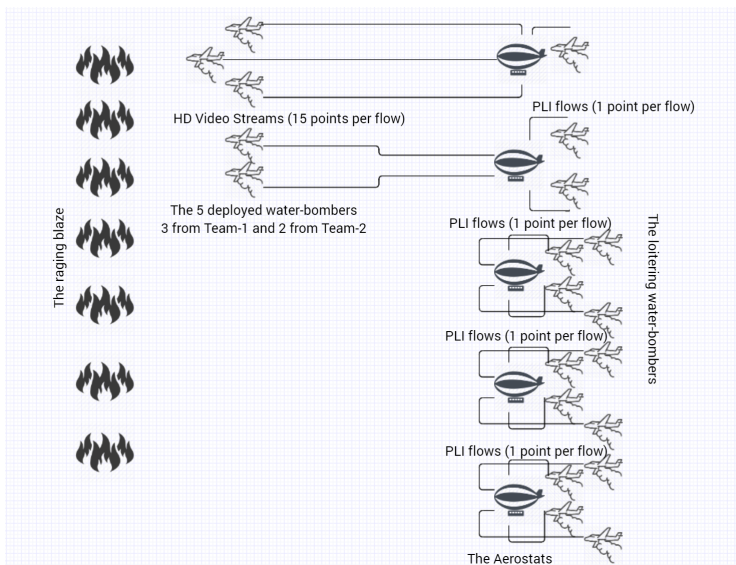


Figure 18: The logistics of the SC2 Wildfire deployment scenario

BAM! Wireless Network Performance Analysis: SC2 Wildfire (2/2)

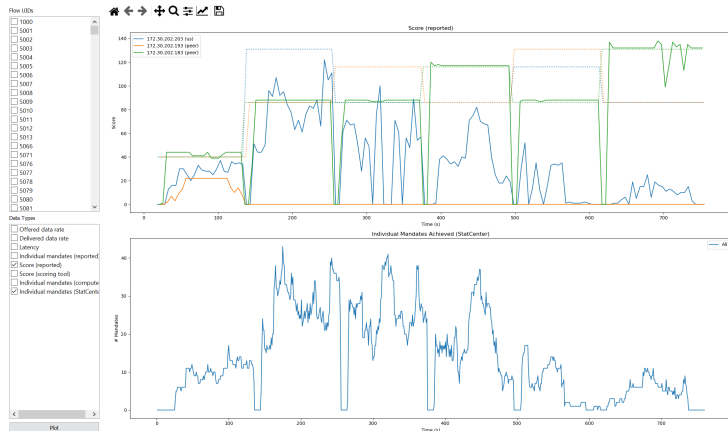


Figure 19: The scores attained by our network: **much better** than the peer in **orange** throughout, **performance comparable** to the peer in **green** in Stages 1 – 3

Condensed Simplification: Spectrum Sensing & Access

- ▶ Focus on spectrum sensing and access in the MAC
- ▶ Centralized deployment
- ▶ Simplified considerations that scale well to real scenarios
- ▶ HMMs and Approx. POMDPs to find optimal policy

Related Work

- ▶ Custom heuristics⁵, HMMs⁶, MABs⁷, RL-agents⁸: Issues
 - ▶ Noise-free [5] obs or Ignored [8] errors in state estimation
 - ▶ Failure to exploit [7] time-frequency correlation structure
 - ▶ Apriori knowledge [8] of this correlation model
 - ▶ Offline estimation [5] of this correlation model
 - ▶ No support ([8], [5]) for tuning throughput and interference

⁵ M. Gao, et. al., "Fast Spectrum Sensing...", 2014 IEEE MilCom

⁶ C. Park, et. al., "HMM Based Channel Status Predictor for Cognitive Radio", 2007 APAC MW Conference

⁷ K. Cohen, et. al., "Restless Multi-Armed Bandits...", 2014 Asilomar

⁸ J. Lundén, et. al., "Multiagent Spectrum Sensing...", IEEE Journal of Selected Topics in Signal Processing

Challenges: Solutions⁹

- ▶ Noisy observation model with Rayleigh fading channels
- ▶ Successfully exploit time-frequency correlation structure
- ▶ No apriori knowledge of this correlation model
- ▶ Online estimation of this correlation model
- ▶ Approximate POMDP with heuristics
- ▶ Support for throughput and interference tuning

⁹ B. Keshavamurthy, N. Michelusi, "Spectrum Sensing in Cognitive Radio Networks via Approximate POMDP", Unpublished, 2020

Signal Model

OFDMA; AWGN observation model; Rayleigh fading channel

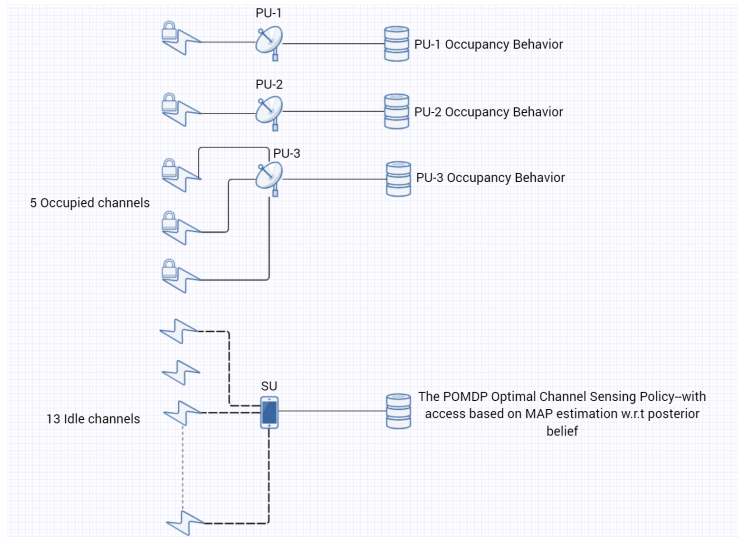


Figure 20: The simplified cognitive radio network under analysis

PU Occupancy Model

$$\mathbb{P}(\vec{B}(i+1) | \vec{B}(i)) = \mathbb{P}(B_1(i+1) | B_1(i)) \prod_{k=2}^K \mathbb{P}(B_k(i+1) | B_k(i), B_{k-1}(i+1))$$

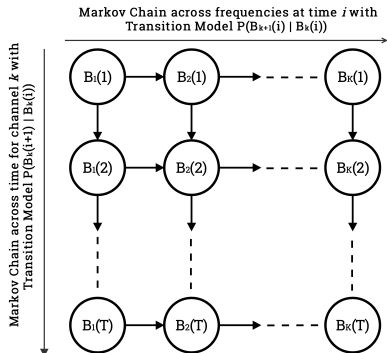


Figure 21: The **time-frequency correlation structure** of the incumbent occupancy behavior

SU Spectrum Sensing Model¹⁰

- ▶ SU can sense at most κ out of K spectrum bands at any given time, with $1 \leq \kappa \leq K$
- ▶ HMM framework:

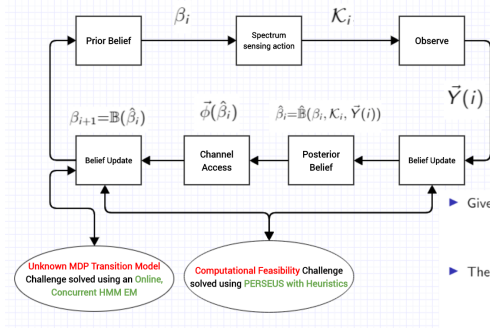
$\vec{Y}(i) = [Y_k(i)]_{k \in \mathcal{K}_i}$ is the observation vector;

$f(\vec{Y}(i)|\vec{B}(i), \mathcal{K}_i) = \prod_{k \in \mathcal{K}_i} f(Y_k(i)|B_k(i))$ is its PDF;

$Y_k(i)|B_k(i) \sim \mathcal{CN}(0, \sigma_H^2 P_{tx} B_k(i) + \sigma_V^2)$ from the signal model

¹⁰ S. Malecki, et. al., "Energy and throughput efficient strategies...", 2011 IEEE 12th International Workshop on Signal Processing Advances in Wireless Communications

POMDP Agent Model (1/2)



The prior belief in time-slot $i + 1$:

$$\beta_{i+1}(\vec{B}'') = \sum_{\vec{B}'} \mathbb{P}(\vec{B}(i+1) = \vec{B}'' | \vec{B}(i) = \vec{B}') \hat{\beta}_i(\vec{B}')$$

The posterior belief:

$$\begin{aligned} \vec{\phi}(\hat{\beta}_i) &= \mathbb{P}(\vec{B}(i) = \vec{B}' | \vec{Y}(i), \mathcal{K}_i, \beta_i) \\ &= \frac{\mathbb{P}(\vec{Y}(i) | \vec{B}', \mathcal{K}_i) \beta_i(\vec{B}')}{\sum_{\vec{B}'' \in \{0,1\}^K} \mathbb{P}(\vec{Y}(i) | \vec{B}'', \mathcal{K}_i) \beta_i(\vec{B}'')} \end{aligned}$$

► Given the posterior belief $\hat{\beta}_i$, we estimate $\vec{B}(i)$ as

$$\vec{\phi}(\hat{\beta}_i) \triangleq \arg \max_{\vec{B} \in \mathcal{B}} \hat{\beta}_i(\vec{B}),$$

► The reward function:

$$R(\vec{B}(i), \hat{\beta}_i) = \sum_{k=1}^K (1 - B_k(i))(1 - \phi_k(\hat{\beta}_i)) - \lambda B_k(i)(1 - \phi_k(\hat{\beta}_i))$$

Figure 22: The POMDP Formulation

POMDP Agent Model (2/2)

- ▶ Exploit the Markovian correlation model¹¹
- ▶ **Goal:** Find optimal spectrum sensing policy that maximizes the infinite-horizon discounted reward:

$$\pi^* = \arg \max_{\pi} V^\pi(\beta) \triangleq \mathbb{E}_\pi \left[\sum_{i=1}^{\infty} \gamma^i R(\vec{B}(i), \hat{\beta}_i) | \beta_0 = \beta \right]$$

- ▶ π^* is the solution to $V^* = \mathcal{H}[V^*]$; **Bellman operator** $V_{t+1} = \mathcal{H}[V_t]$ is

$$V_{t+1}(\beta) = \max_{\mathcal{K} \in \mathcal{A}} \sum_{\vec{B} \in \mathcal{B}} \beta(\vec{B}) \mathbb{E}_{\vec{Y}|\vec{B}, \mathcal{K}} \left[R(\vec{B}, \hat{\mathbb{B}}(\beta, \mathcal{K}, \vec{Y})) + \gamma V_t(\mathbb{B}(\hat{\mathbb{B}}(\beta, \mathcal{K}, \vec{Y}))) \right], \forall \beta$$

¹¹S. Mosleh, et. al., "Performance analysis of the Neyman-Pearson fusion center...", IEEE EUROCON 2009

The Parameter Estimator¹²

- ▶ MLE problem:

$$\vec{\theta}^* = \arg \max_{\vec{\theta}} \log \left(\sum_{\mathbf{B}} \mathbb{P}(\mathbf{B}, \mathbf{Y} | \vec{\theta}) \right)$$

- ▶ The Baum-Welch algorithm (EM for HMMs):

E-step: $Q(\vec{\theta} | \vec{\theta}^{(t)}) = \mathbb{E}_{\mathbf{B} | \mathbf{Y}, \vec{\theta}^{(t)}} \left[\log \left(\mathbb{P}(\mathbf{B}, \mathbf{Y} | \vec{\theta}^{(t)}) \right) \right]$

M-step: $\vec{\theta}^{(t+1)} = \arg \max_{\vec{\theta}} Q(\vec{\theta} | \vec{\theta}^{(t)})$

¹²W. Turin, "Map decoding using the EM algorithm", 1999 IEEE 49th Vehicular Technology Conference

PERSEUS¹³ (1/2)

- ▶ **Initial exploration:** $\tilde{\mathcal{B}}$
- ▶ **Goal:** Improve the value of all the belief points in $\tilde{\mathcal{B}}$ by updating the value of only a subset of these belief points, chosen iteratively at random
- ▶

$$V_t(\beta) \approx \beta \cdot \vec{\alpha}_t^{u^*}, \quad u^* = \arg \max_{u \in \{1, 2, \dots, |\tilde{\mathcal{B}}|\}} \beta \cdot \vec{\alpha}_t^u, \quad \beta \cdot \vec{\alpha} = \sum_{\vec{B}} \beta(\vec{B}) \vec{\alpha}(\vec{B})$$

¹³ T.J. Spaan, et. al., "Perseus: Randomized Point-based Value Iteration for POMDPs", Journal of Artificial Intelligence Research, 2005

PERSEUS (2/2)

- ▶ Initialization: $\tilde{\mathcal{U}} = \tilde{\mathcal{B}}$
- ▶ Backup:
 - ▶ Find a new hyperplane associated with randomly chosen β_u :

$$\vec{\alpha}_{t+1}^u = \Xi_{\mathcal{K}_{t+1}^u}^u, \quad \mathcal{K}_{t+1}^u = \arg \max_{\mathcal{K} \in \mathcal{A}} \beta_u \cdot \Xi_{\mathcal{K}}^u$$

$$\begin{aligned} \Xi_{\mathcal{K}}^u(\vec{B}) = & \mathbb{E}_{\vec{Y}|\vec{B}, \mathcal{K}} \left[R(\vec{B}, \hat{\mathbb{B}}(\beta_u, \mathcal{K}, \vec{Y})) + \right. \\ & \left. \gamma \sum_{\vec{B}'} \mathbb{P}(\vec{B}(i+1) = \vec{B}' | \vec{B}(i) = \vec{B}) \Xi_{\mathcal{K}, \vec{Y}}^u(\vec{B}') \right] \end{aligned}$$

Future value function: $\Xi_{\mathcal{K}, \vec{Y}}^u = \arg \max_{\alpha_t^{u'}, u' \in \{1, 2, \dots, |\tilde{\mathcal{B}}|\}} \mathbb{B}(\hat{\mathbb{B}}(\beta_u, \mathcal{K}, \vec{Y})) \cdot \alpha_t^{u'}$

- ▶
- ▶ $\tilde{\mathcal{U}} \leftarrow \tilde{\mathcal{U}} \setminus \{\beta_u\} \setminus \{\beta' \in \tilde{\mathcal{U}} : \beta' \cdot \vec{\alpha}_{t+1}^u \geq V_t(\beta')\}$
- ▶ Backup termination: $\tilde{\mathcal{U}} = \emptyset$
- ▶ PERSEUS Termination: $|V_{t+1}(\beta) - V_t(\beta)| < \epsilon, \forall \beta \in \tilde{\mathcal{B}}, \epsilon > 0$

PERSEUS Heuristics

- ▶ **Fragmentation:** smaller, independent sets of correlated channels governed by incumbent-specific behavior
- ▶ **Belief Update Simplification:** Hamming distance filter to avoid iterating over all possible states

Simulation setup

- ▶ $\vec{p} = [p_{00}=0.1, p_{01}=p_{10}=0.3, p_{11}=0.7]^\top$ and $\vec{q} = [q_0=0.3, q_1=0.8]^\top$

- ▶ $\kappa=6$

- ▶

$$C^{\text{SU}} = \frac{1}{T} \sum_{i=1}^T \sum_{k=1}^K R_{\text{SU}} \cdot \mathcal{I} \left(\text{SINR}_{\text{SU}}(k, i) \geq 2^{R_{\text{SU}}/\text{BW}} - 1 \right),$$

$R_{\text{SU}}=0.6\text{Mbps}$

- ▶

$$C^{\text{PUs}} = \frac{\sum_{i=1}^T \sum_{k=1}^K R_{\text{PU}} B_k(i) \mathcal{I} \left(\text{SINR}_{\text{PU}}(k, i) \geq 2^{R_{\text{PU}}/\text{BW}} - 1 \right)}{\sum_{i=1}^T \sum_{k=1}^K B_k(i)},$$

$R_{\text{PU}}=0.9\text{Mbps}$

- ▶ $\gamma=0.9, \epsilon=10^{-5}, \text{Hamming distance filter metric}=3$

Numerical Evaluations (1/6)

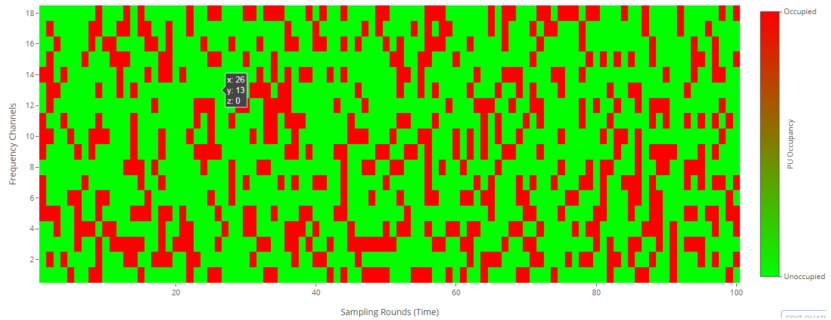


Figure 23: The time-frequency incumbent occupancy behavior assuming independence across both frequency and time

Numerical Evaluations (2/6)

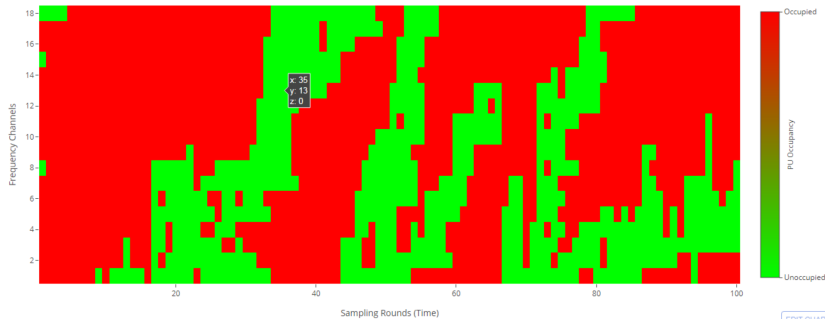


Figure 24: The time-frequency incumbent occupancy behavior assuming a Markovian correlation across both frequency and time

Numerical Evaluations (3/6)

Detection Accuracy v/s $P(\text{Occupied} \mid \text{Idle})$ for 18 channels at $P(X_i = 1) = 0.6$ with varying uniform channel sensing strategies

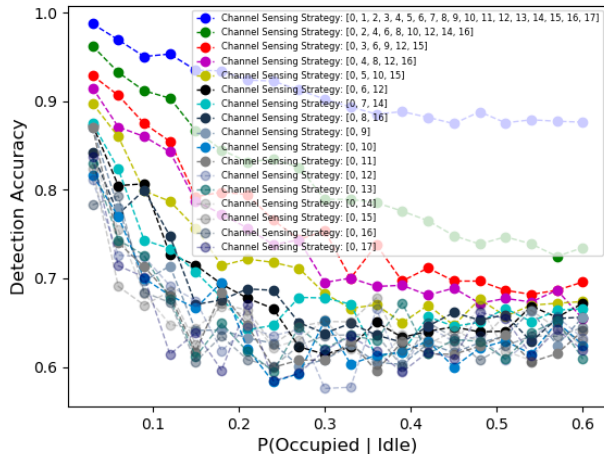


Figure 25: Single Markov chain across channels: Effect of channel sensing limitations, channel correlation, and sensing strategies on estimation/detection accuracy

Numerical Evaluations (4/6)

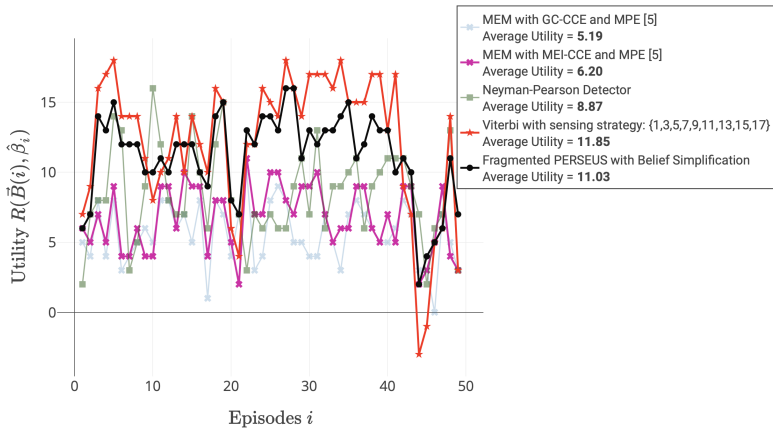


Figure 26: The comparison of the utility obtained by our framework per time-slot against that obtained by other schemes in the state-of-the-art

[5]: M. Gao, et. al., "Fast Spectrum Sensing...", 2014 IEEE MilCom

[Viterbi]: C. Park, et. al., "HMM Based Channel Status Predictor for Cognitive Radio", 2007 APAC MW Conf

[NPD]: S. Mosleh, et. al., "Performance analysis of the Neyman-Pearson fusion center...", IEEE EUROCON 2009

Numerical Evaluations (5/6)

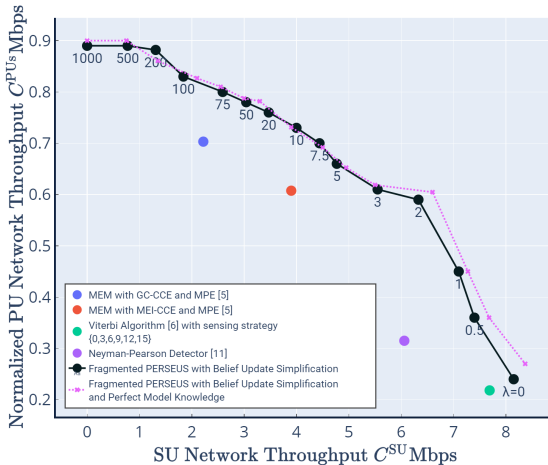


Figure 27: Evaluation of C^{SU} versus C^{PUs} for different values of the penalty λ ; comparison with state-of-the-art

[5]: M. Gao, et. al., "Fast Spectrum Sensing...", 2014 IEEE MilCom

[6]: C. Park, et. al., "HMM Based Channel Status Predictor for Cognitive Radio", 2007 Asia-Pacific MW Conf

[11]: S. Mosleh, et. al., "Performance analysis of the Neyman-Pearson fusion center...", IEEE EUROCON 2009

Numerical Evaluations (6/6)

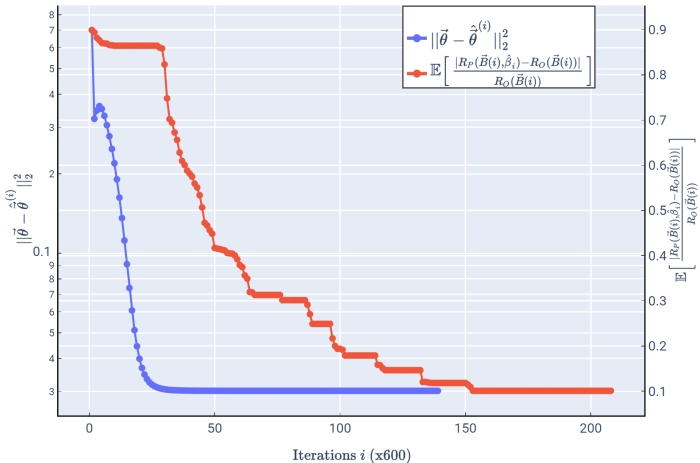


Figure 28: Convergence of: MSE of the EM algorithm to estimate $\vec{\theta}$; and Normalized sub-optimal gap of the fragmented PERSEUS algorithm with belief update simplification

POMDP Access Policy Implementation

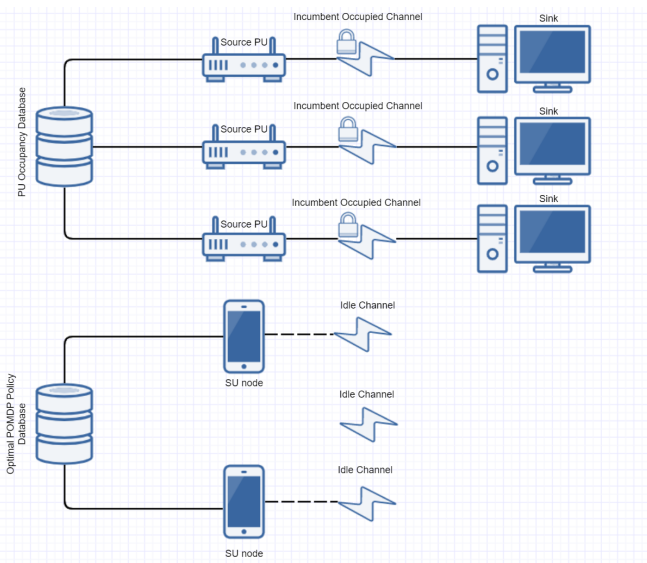


Figure 29: The distributed ad-hoc network consisting entirely of **ESP32** radios serving as PU sources, sinks, & SUs

Time-slotted Detection Accuracy¹⁴

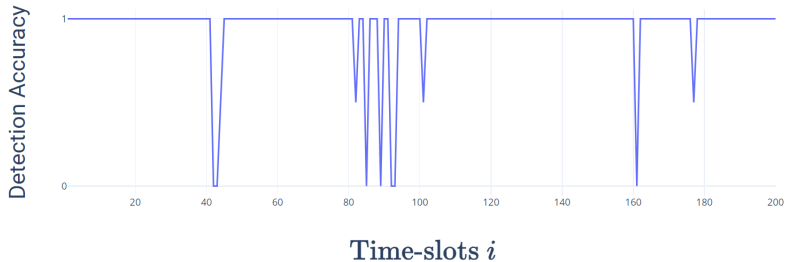


Figure 30: The time-slotted **detection accuracy** of the cognitive radios (SUs) in this distributed ad-hoc network of ESP32 radios over 2.4GHz WiFi channels

¹⁴ Recent Update: Need to compare this performance with a situation where incumbent occupancy independence is assumed across time and frequency

Q&A

Thank you